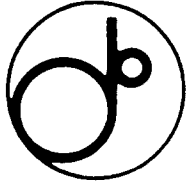


EE

KEK P 93-158
SW 9409



KEK Preprint 93-158
December 1993
A

Proof-of-Principle Experiments of Laser Wake-Field Acceleration

K. NAKAJIMA, T. KAWAKUBO, H. NAKANISHI, A. OGATA, Y. KATO, Y. KITAGAWA,
R. KODAMA, K. MIMA, H. SHIRAGA, K. SUZUKI, K. YAMAKAWA, T. ZHANG,
Y. SAKAWA, T. SHOJI, Y. NISHIDA, N. YUGAMI, M. DOWNER, D. FISHER,
B. NEWBERGER and T. TAJIMA

CERN LIBRARIES, GENEVA



P00021321

Submitted to Phys. Rev. Lett.

National Laboratory for High Energy Physics, 1993

KEK Reports are available from:

Technical Information & Library
National Laboratory for High Energy Physics
1-1 Oho, Tsukuba-shi
Ibaraki-ken, 305
JAPAN

Phone: 0298-64-1171
Telex: 3652-534 (Domestic)
(0)3652-534 (International)
Fax: 0298-64-4604
Cable: KEK OHO
E-mail: LIBRARY@JPNKEKVX (Bitnet Address)
library@kekvax.kek.jp (Internet Address)

Proof-of-Principle Experiments of Laser Wake-Field Acceleration

K. Nakajima, T. Kawakubo, H. Nakanishi, and A. Ogata

National Laboratory for High Energy Physics, Tsukuba, Ibaraki, Japan

Y. Kato, Y. Kitagawa, R. Kodama, K. Mima, H. Shiraga,

K. Suzuki, K. Yamakawa and T. Zhang

Institute of Laser Engineering, Osaka University, Osaka, Japan

Y. Sakawa, and T. Shoji

Plasma Science Center of Nagoya University, Nagoya, Japan

Y. Nishida, and N. Yugami

Utsunomiya University, Utsunomiya, Japan

M. Downer, D. Fisher, B. Newberger, and T. Tajima

The University of Texas at Austin, Austin, Texas, U.S.A.

ABSTRACT

The principle of laser wakefield particle acceleration has been tested by the Nd:glass laser system providing a short pulse with a power of 10 TW and a duration of 1 ps. Electrons accelerated up to 18 MeV/c have been observed by injecting 1 MeV/c electrons emitted from a solid target by an intense laser impact. The corresponding field gradient achieved is 1.7 GeV/m. This work constitutes the first result of the laser wakefield acceleration.

PACS numbers: 52.35.Mw, 52.40.Nk, 52.75.Df

Recently there has been a great interest in laser-plasma accelerators as possible next generation particle accelerators because of their potential for ultrahigh accelerating gradients and compact size compared with conventional accelerators. It is

known that the laser pulse is capable of exciting a plasma wave propagating at a phase velocity close to the velocity of light by means of beating two-frequency lasers or an ultrashort laser pulse [1]. These schemes came to be known as the Beat Wave Accelerator (BWA) for beating lasers or as the Laser Wakefield Accelerator (LWFA) for a short pulse laser. Experimental activities around the world have focused on the BWA scheme using CO₂ and Nd:glass lasers [2], primarily because of lack of intense ultrashort pulse lasers till recently. A possible advantage in the BWA is efficient excitation of plasma waves due to resonance between the beat frequency of two lasers and the plasma frequency. On the other hand, a fine adjustment of the beat frequency with the plasma frequency is necessary. In the meantime, the LWFA does not rely on the resonant excitation of plasma waves so that a fine tuning of the plasma density is not absolutely necessary. Excitation of the plasma wave becomes more efficient in the LWFA than the BWA as the laser intensity increases over $\sim 10^{18}$ W/cm² for a Nd:glass laser. Furthermore a new prospect of the LWFA are proposed, that is called "self-modulated-LWFA" [3] in which the self-modulation of the laser pulse is accompanied by the resonant excitation of wakefields behind the pulse. If practical and controllable, this scheme will have significant advantages in laser-plasma accelerators. In the LWFA scheme, however, no experiment is reported on the wakefield excitation and its acceleration of particles to date. This letter reports a first experimental result on the laser wakefield acceleration and on evidence of more efficient acceleration mechanism.

To estimate the amplitude of wakefields in a plasma excited by an intense short laser pulse, we employed a fluid model of the plasma dynamics, assuming a cold plasma of electron fluid and stationary ions. The momentum, continuity and Poisson's equations are linearized to result in a simple harmonic oscillator equation for the wake potential of the electron fluid driven by the ponderomotive force of the laser

field. An analytical solution for the wake potential is obtained for transversely and longitudinally Gaussian pulse envelope [4]. The axial and radial wakefields are calculated from the wake potential resulted from the density oscillation with the plasma frequency $\omega_p = \sqrt{4\pi e^2 n_e/m_e}$ for the ambient density n_e of the plasma electrons. The maximum amplitude of the axial wakefield is achieved at the plasma wavelength $\lambda_p = \pi\sigma_z: (eE_z)_{\max} \simeq 1.3m_e c^2 a_0^2/\sigma_z$, where σ_z is the rms pulse length and a_0 is the normalized vector potential of the laser field given by $a_0^2 = 0.73 \times 10^{-18} I \lambda_0^2$ for the peak intensity I in units of W/cm^2 , the laser wavelength $\lambda_0 = 2\pi c/\omega_0$ in units of μm , and the laser frequency ω_0 . The density response and the axial wakefield excited by a laser pulse with a pulse duration of 1 ps (FWHM) are shown in Fig. 1 as well as evolution of the plasma electron density. Assuming a Gaussian beam propagation of the laser pulse in a fairly underdense plasma, the longitudinal wakefield excited behind a Gaussian laser pulse is written as

$$eE_z(r, z) \simeq \frac{n_e c^2 \epsilon_0}{Z_R [1 + (z/Z_R)^2]} \exp\left(-\frac{2r^2}{R_0^2 [1 + (z/Z_R)^2]}\right) \cos \psi, \quad (1)$$

where Z_R is the Rayleigh length, $Z_R = \pi R_0^2/\lambda_0$, R_0 the radius of the beam waist, $\psi = k_p z - \omega_p t$, $k_p = \omega_p/v_p$, v_p is the phase velocity of the plasma wave equal to the group velocity of the laser pulse in a plasma given by $v_p = c\sqrt{1 - \omega_p^2/\omega_0^2}$, and

$$\epsilon_0 = \frac{\Omega_0 P}{\sqrt{\pi} m_e^2 c^4} \left(\frac{\lambda_0}{\lambda_p}\right) k_p \sigma_z \exp\left(-\frac{k_p^2 \sigma_z^2}{4}\right), \quad (2)$$

with the vacuum resistivity Ω_0 (377 ohms). Thus equations of electron motion are given by

$$\frac{d\mathbf{p}}{dt} = -e\mathbf{E}, \quad \frac{d\psi}{dt} = \omega_p \left(\frac{v_z}{v_p} - 1\right), \quad (3)$$

where \mathbf{p} is the momentum of electron and $v_z = dz/dt$. The maximum energy gained by a synchronized electron with velocity equal to the phase velocity of the plasma

wave is obtained by integrating the axial wakefield along the laser beam axis as $\Delta E = \pi m_e c^2 \epsilon_0 \cos \psi_s$ for the synchronous phase ψ_s of an electron trapped by the wave potential. Thus the energy spectrum of accelerated electrons would be continuously distributed up to the maximum energy. Using a laser pulse with a FWHM duration τ_L in units of ps at $\lambda_0 = 1.052 \mu\text{m}$, the maximum energy gain is expected to achieve $(\Delta E)_{\max} \simeq 1.2P/\tau_L$ MeV for the laser peak power P in units of TW.

In this experiment, the laser pulse is delivered by the Nd:glass laser system [5] capable of generating the peak power up to 30 TW with a pulse duration of 1 ps. This laser system is based on the technique of chirped pulse amplification [6]. A low energy pulse of 20 nJ with 130 ps duration from the mode-locked oscillator is passed through a single mode fiber of a 1.85 km length to produce a linear frequency chirp. The long linearly chirped pulse with 450 ps duration and 4 nm bandwidth at exit of the fiber is split into two pulses each of which is amplified to the maximum energy of 40 J through each broad bandwidth amplifier-chain. One of amplified pulses with 200 ps duration and 1.8 nm bandwidth is compressed to 1 ps duration by a pair of gratings. The other uncompressed pulse is focused on the solid target to produce an electron beam.

The experimental setup is schematically shown in Fig. 2. The laser beam with a 140 mm diameter from the compression stage is focused by a 3.1 m focal length lens of $f/22$ into the vacuum chamber filled with a He gas to a spot size of 80 μm . The peak intensity of the order of 10^{17} W/cm² can be achieved so that a fully ionized plasma can be created in a fast time scale (≤ 10 fs) due to the tunneling ionization process. The threshold intensity for the onset of tunneling ionization is 8.8×10^{15} W/cm² for He²⁺ ion [7]. With a 10 TW laser pulse focused into the He gas, the fully ionized plasma can be produced over more than 60 mm around the beam waist. The compressor grating-pair, the 10° mirror and the focusing lens are installed in

the vacuum vessel connected to the vacuum chamber for the acceleration experiment. These vacuum chambers are evacuated down to $\sim 10^{-5}$ Torr with two turbo molecular pumps. For creation of a low density plasma, a gas was statically filled with the flow controlled valve. For the high density plasma experiment, a He gas was filled with the supersonic gas jet injector.

Electrons for acceleration are produced from an aluminum solid target irradiated by the amplified 200 ps laser pulse. The P -polarized laser beam with 140 mm diameter is focused with a 1.6 m focal length lens to a spot size of 40 μm diameter on the aluminum rod of 6 mm diameter. The peak intensity then exceeds 10^{16} W/cm² for 20 J irradiation which is sufficient to induce stimulated Raman scattering instabilities. The target rod of 60 mm length is mounted on the plunger head inside the vacuum chamber and vertically shifted by a 0.5 mm step in each shot to replace an ablated surface into a fresh surface shot by shot. Hot electrons emitted from the target are injected into the waist of the 1 ps pulse laser beam through the 90° bending magnet with appropriate edge angles so as to achieve double focusing of an electron beam. Since the electron beam length is as short as the 200 ps laser pulse duration, the optical path length of the 200 ps laser pulse is adjusted so that the 1 ps laser pulse should overlap with electrons at the focus within ± 100 ps. Electrons trapped by wakefields are accelerated in the beam waist of twice the Rayleigh length, ≈ 10 mm. The momentum of electron is analyzed by the dipole field of the magnetic spectrometer placed in the exit of the interaction chamber. This spectrometer covers the momentum range of 6–19.5 MeV/c at the dipole field of 3.9 kG. Upon exiting the vacuum chamber through a 100 μm thick Capton window, electrons are detected by the array of 32 scintillation counters each of which is assembled with a 3 mm thick, 10 mm wide, 60 mm long plastic scintillator coupled to a 1/2-in. photomultiplier tube. Pulse heights of the detector are measured by the fast multichannel CAMAC ADCs

gated by the trigger pre-pulse in coincidence with the laser pulse. The momentum resolution of the spectrometer is typically 1.0 MeV/c per channel at the 3.9 kG bending field. The background x rays are detected by 4 scintillation counters placed around the vacuum chamber to monitor electron intensity. The vacuum chamber is shielded by 4 mm thick lead sheets to reduce the flux of background x rays. The back of the detector is entirely surrounded by 50 mm thick lead bricks so that the background signal levels can be reduced to be less than a few counts for all ADC channels.

In the beginning of this experiment, the electron production has been carried out by using only the 200 ps laser pulse. The momentum distribution of produced electrons was measured with the spectrometer for the injection bending field set to 0.5, 1.0, and 2.0 MeV/c. The data are summarized in Fig. 3. The flux of electrons above 2 MeV/c (≈ 1.6 MeV kinetic energy) is negligibly small. A number of electrons along with numerous x rays were produced above the pulse energy of 20 J corresponding to $\sim 10^{16}$ W/cm². This result implies that energetic electrons are produced by Raman forward scattering instability [8]. For the injection bending field set to 340 G, the number of hot electrons with momentum of 0.88 ± 0.3 MeV/c was estimated to be $\sim 10^4$ in the interaction region.

In the acceleration experiment the injection bending field was set to 1 MeV/c. Such electron production in the laser shots was identified from signal levels in x-ray monitoring detectors. The momentum distribution of electrons was measured for 8 TW focused into a static fill of 50 mTorr of He gas as shown in Fig. 4. The electron density of a fully ionized plasma is 3.5×10^{15} cm⁻³ at this pressure. The spectrum of electrons measured at 50 mTorr is distinguished from the data measured for 7 TW injected into an evacuated chamber at 5.2×10^{-5} Torr. No energetic electrons above 2 MeV/c were observed when both the 200 ps pulse and the 1 ps pulse were injected in

the evacuated chamber. The momentum spectrum of accelerated electrons has been estimated by integrating equations of electron motion Eq. (3) as shown in Fig. 5. The simulation results are in good agreement with the experimental data points obtained for the 8 TW injection. The data obtained from the evacuated condition (no plasma) are also roughly in agreement with the momentum spectrum of injected electrons assuming a Gaussian distribution with the mean momentum 0.9 MeV/c and the rms spread 0.3 MeV/c. The simulation indicates that injected electrons were accelerated by the excited plasma wave of the peak accelerating gradient of 0.7 GeV/m.

In the high plasma density experiment we observed several data points contributed by electrons accelerated up to higher momenta than 6 MeV/c when the gas was injected at the back-pressure of 8 atm. The observed data are shown in Fig. 5. Significant signal levels in the momentum spectrum were detected when electrons were injected. With no electrons injected, the detectable signal levels were as small as the background signals. It implies that there was no significant contribution to detectable signals due to self-trapping of the background plasma electrons and x-ray emissions in the plasma. The highest momentum of the accelerated electrons was 17.7 ± 0.5 MeV/c. This indicates the average accelerating gradient of more than 1.7 GeV/m. Since the linear plasma fluid theory can not predict the observed spectrum of accelerated electrons for a rather low power of 3 TW, it is suggested that more efficient excitation of plasma waves may be caused by highly nonlinear effects. A rough estimate of electron acceleration suggests that the maximum amplitude of excited wakefield should be as high as ~ 10 GV/m at the plasma density of $\sim 10^{18}$ cm $^{-3}$ to produce the momentum spectrum electrons observed in the experiment. The self-modulation of a laser pulse has been predicted to excite accelerating electric fields in excess of 100 GV/m around such plasma density [3]. The instability analysis based on the relativistic self-focusing as well as the near-forward Raman instability gives an

estimate of the time required for a structural modulation of the laser pulse to appear as $t = 4T_R / (k_p L a_0^2 c^2 R^2)$, where $T_R = ZR/c$ is the Rayleigh time for the length L and the radius R of a pulse [9]. It implies that the self-modulation of a laser pulse develops in time $t = 0.15T_R$ fast enough to generate enhanced wakefields for the experimental parameters with $a_0 = 0.3$.

In conclusion we have demonstrated that electrons injected into a laser-produced plasma are accelerated by wakefields excited by a short laser pulse. We report the first test of the laser wakefield acceleration mechanism. The momentum spectrum of accelerated electrons has been found to be well identified from simulation results and comparison with no plasma experiment in the linear wakefield regime. In the nonlinear regime we have observed more energetic electrons accelerated up to 18 MeV/c close to the detection limit of the spectrometer. The observation implies that instabilities associated with the relativistic self-focusing and the forward Raman scattering may cause excitation of enhanced wakefields.

The authors would like to acknowledge supports from Professors H. Sugawara and Y. Kimura at the National Laboratory for High Energy Physics (KEK) and the approval of this work and the technical support from Professor S. Nakai and the laser group at the Institute of Laser Engineering in Osaka University. The work was partly supported by JSPS, NSF, U.S. DOE grants and Grant-in-Aid from Ministry for Education, Science and Culture of Japan.

REFERENCES

- [1] T. Tajima and J.M. Dawson, *Phys. Rev. Lett.*, **43**, 267 (1979); L. M. Gorbunov and V. I. Kirsanov, *Zh. Eksp. Teor. Fiz.* **93**, 509 (1987) [*Sov. Phys. JETP* **66**, 290 (1987)]; P. Sprangle et al., *Appl. Phys. Lett.* **53**, 2146 (1988)

FIGURE CAPTIONS

- [2] C. E. Clayton et al., Phys. Rev. Lett. **54**, 2343 (1985); N. A. Ebrahim, Phys. Canada **45**, 178 (1989); A. E. Dangor et al., Phys. Scr. **T30**, 107 (1990); Y. Kitagawa et al., Phys. Rev. Lett. **68**, 321 (1992); F. Amironov et al., Phys. Rev. Lett. **68**, 3710 (1992); C. E. Clayton et al., Phys. Rev. Lett. **70**, 37 (1993)
- [3] N. E. Andreev et al., Zh. Eksp. Teor. Fiz. **55**, 551 (1992) [JETP Lett., **55**, 571 (1992)]; E. Esarey et al., Phys. Fluids B **5**, 2690 (1993).
- [4] K. Nakajima, Phys. Rev. A, **45**, 1149 (1992).
- [5] K. Yamakawa et al., Opt. Lett., **16**, 1593 (1991).
- [6] P. Maine et al., IEEE J. Quantum Electron. **QE-24**, 398 (1988).
- [7] M.V. Ammosov, N.B. Delone and V.P. Krainov, Zh. Eksp. Teor. Fiz., **91**, 2008 (1986) [Sov. Phys. JETP **64**, 1191 (1986)]; B.M. Penetrante and J.N. Bardsley, Phys. Rev. A, **43**, 3100 (1991).
- [8] C. Joshi et al., Phys. Rev. Lett., **47**, 1285 (1981); K. Estabrook and W. L. Krueer, Phys. Fluids **26**, 1892 (1983); S. Athal et al., Phys. Fluids, **30**, 3825 (1987).
- [9] T. M. Antonsen, Jr., and P. Mora, Phys. Rev. Lett., **69**, 2204 (1992).

Fig. 1. Evolution of the electron density n_e , the density perturbation n and the axial electric field E_z excited by a 1 ps Nd:glass laser pulse of the peak intensity 10^{18} W/cm².

Fig. 2. Schematic of the experimental setup.

Fig. 3. Momentum distributions of electrons produced by the 200 ps laser pulse at the injection bending field set to 0.5, 1.0, and 2.0 MeV/c.

Fig. 4. Momentum spectrum of accelerated electrons in a static fill of He gas at 50 mTorr and in the evacuated chamber. The solid line shows the momentum spectrum expected from the simulation of electron acceleration due to the wake-fields excited by a 8 TW laser pulse. The dashed line shows the momentum spectrum of injected electrons.

Fig. 5. Momentum spectrum of accelerated electrons in a He gas jet at 8 atm.

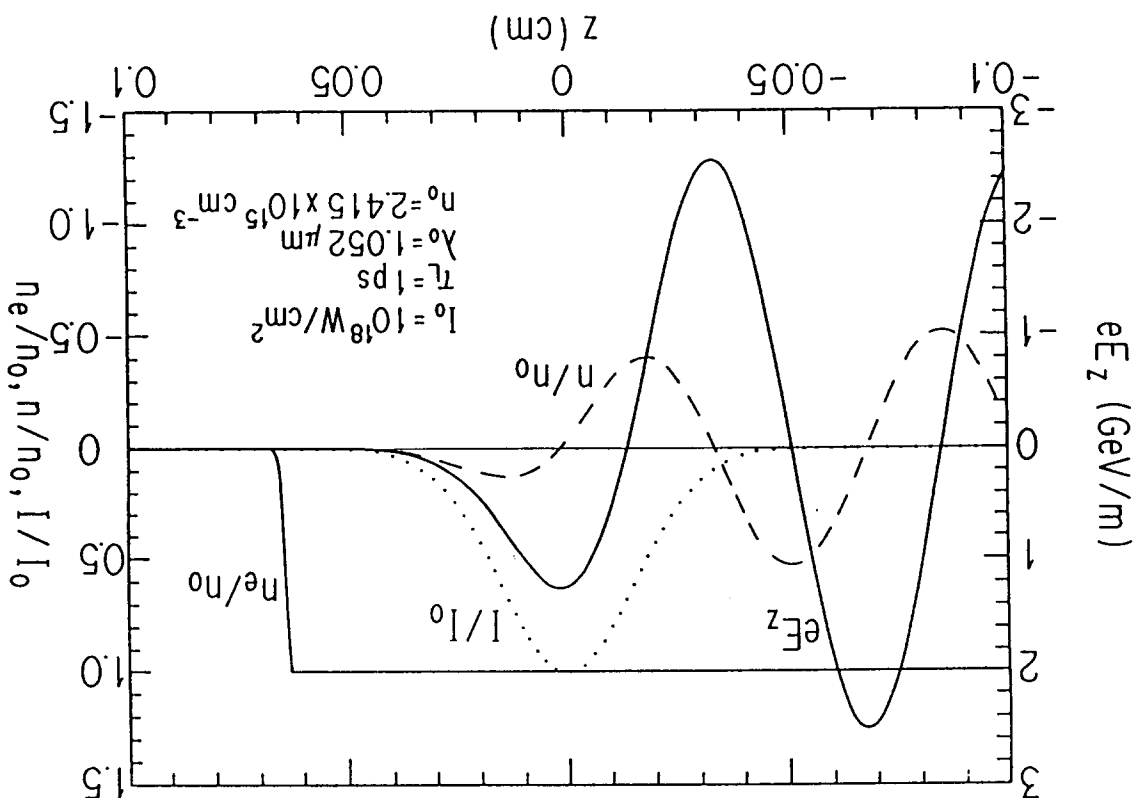


Fig. 1. Evolution of the electron density n_e , the density perturbation n and the axial electric field E_z excited by a 1 ps Nd:glass laser pulse of the peak intensity 10^{18} W/cm^2 .

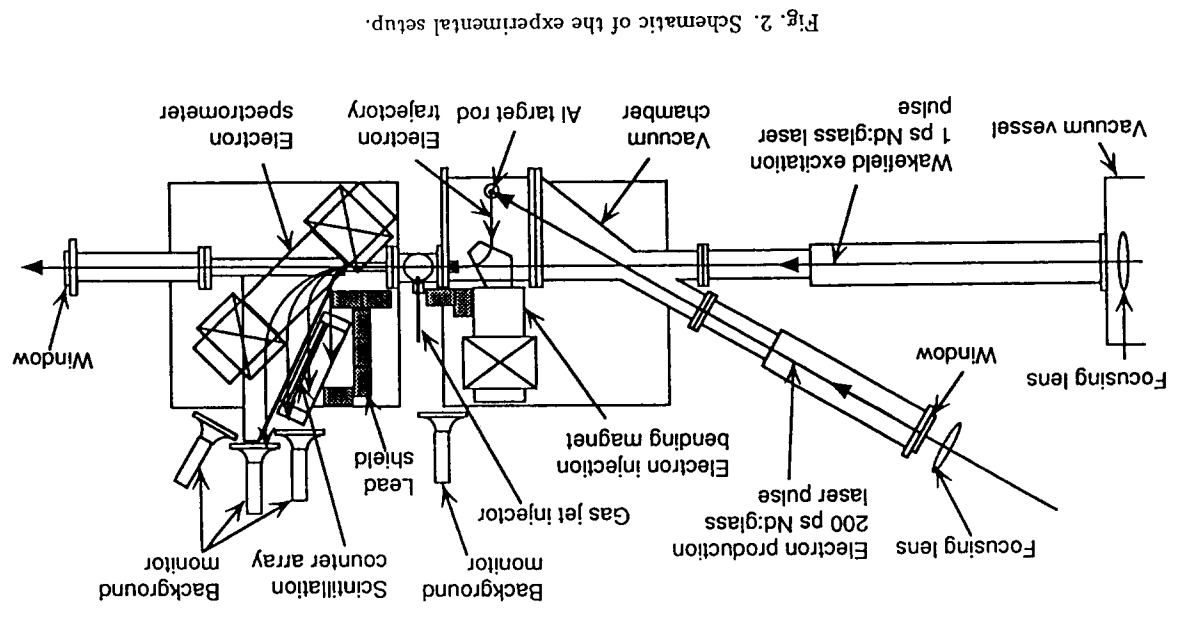


Fig. 2. Schematic of the experimental setup.

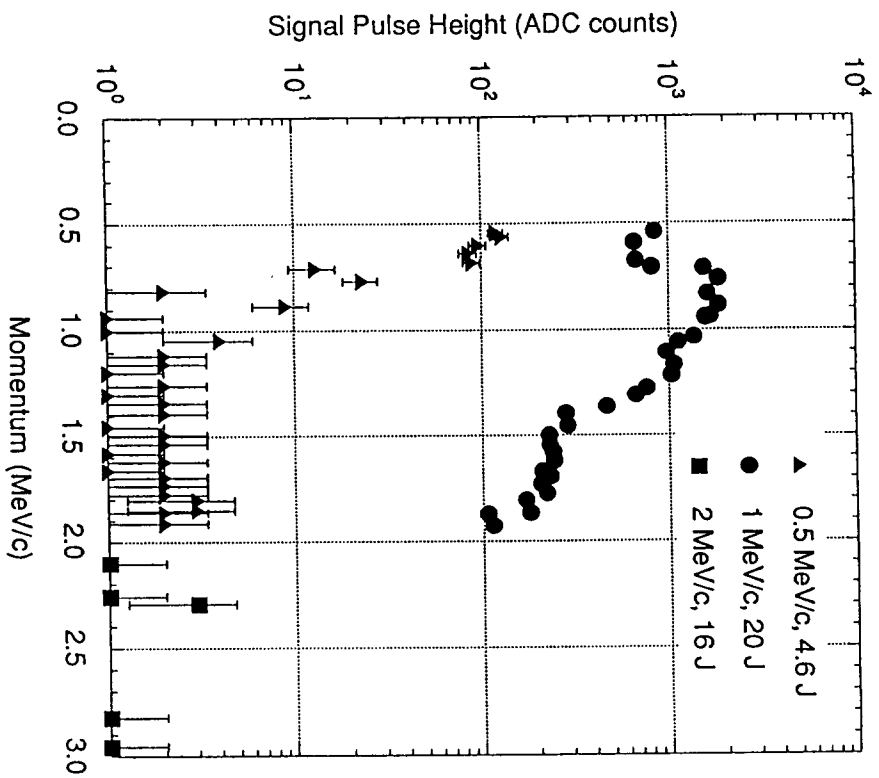


Fig. 3. Momentum distributions of electrons produced by the 200 ps laser pulse at the injection bending field set to 0.5, 1.0, and 2.0 MeV/c.

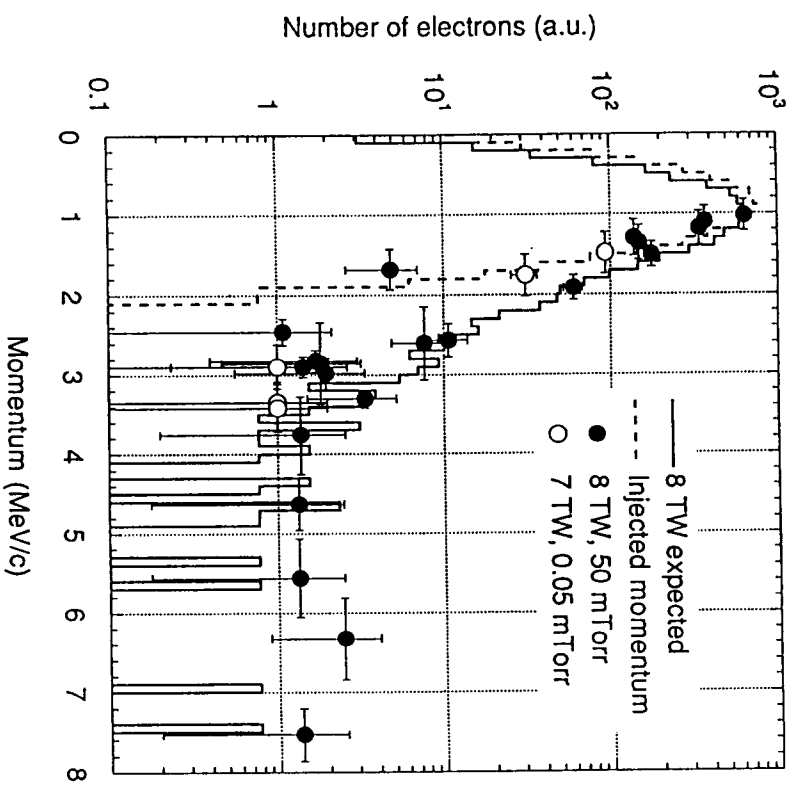


Fig. 4. Momentum spectrum of accelerated electrons in a static fill of He gas at 50 mTorr and in the evacuated chamber. The solid line shows the momentum spectrum expected from the simulation of electron acceleration due to the wake-fields excited by a 8 TW laser pulse. The dashed line shows the momentum spectrum of injected electrons.

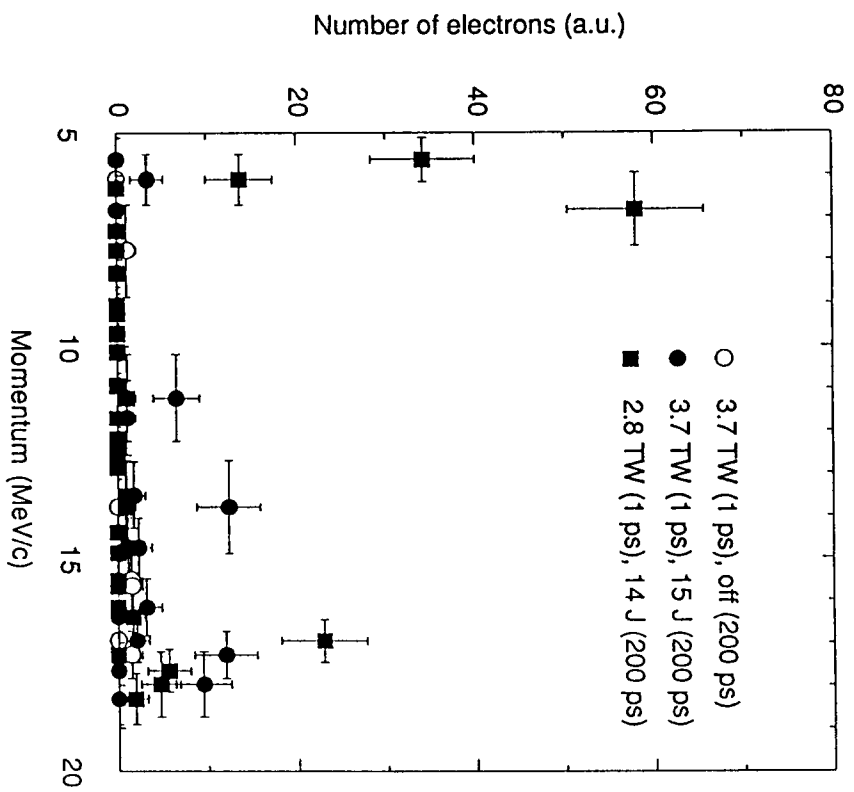


Fig. 5. Momentum spectrum of accelerated electrons in a He gas jet at 8 atm.